Polyhedron 221 (2022) 115865

Contents lists available at ScienceDirect

Polyhedron

journal homepage: www.elsevier.com/locate/poly

Sulfonamides with hydroxyphenyl moiety: Synthesis, structure, physicochemical properties, and ability to form complexes with Rh(III) ion

Małgorzata Gawrońska [a,*], Mateusz Kowalik [a], Joanna Duch [a], Katarzyna Kazimierczuk [b], Mariusz Makowski [a]

[a] University of Gdańsk, Faculty of Chemistry, Wita Stwosza 63, 80-308 Gdańsk, Poland
[b] Gdańsk University of Technology, Faculty of Chemistry, Gabriela Narutowicza 11/12, 80-233 Gdańsk, Poland

ARTICLE INFO

Keywords:
Rhodium(III) ion
Complexes
Sulfa drug

ABSTRACT

Sulfonamides are the first successfully synthesized antimicrobial drugs. The mechanism of sulfonamides' antimicrobial action involves competitive inhibition of folic acid synthesis and prevention of the growth and reproduction of bacteria. Even though they have been applied in therapy for more than 75 years, sulfonamides are still the drugs of choice for the treatment of various diseases. The aim of this work was to synthesize and characterize two new sulfonamides hydroxyphenyl moiety and investigate their ability to form complexes with Rh(III). The results of recent studies indicate an increased interest in the application of potential platinum-group metal ion complexes as an alternative, promising candidates for anticancer and antimicrobial drugs.

1. Introduction

Amides of sulfonic acid are structural motifs that commonly appear in synthetic drugs. The antibacterial properties of the first synthesized sulfonamide were discovered by Gerhard Domagek [1], which led to the development of "sulfa drugs". Since then, an abundance of sulfonamide derivatives has been reported. Besides the well-known antibacterial effect [2] they exhibit anticancer [3], diuretic [4], hypoglycemic [5], anti-inflammatory [6], or carbonic anhydrase inhibitory [7] properties. Different pharmacological drugs with a variety of biological activity are based on the structure of a very simple compound, such as sulfanilamide, including sulfamethoxazole – antibacterial [8]; furosemide – diuretic [9]; glibenclamide – hypoglycemic [10]; diclofenamide – carbonic anhydrase inhibitor [11]; amprenavir – anti-AIDS [12]; sulfasalazine – rheumatoid arthritis [13] (Fig. 1).

However, the emergence of drug resistance that we all struggle with, the frustrating treatment of patients, forces us to look for newer drugs that can break this phenomenon. Sulfonamides have attracted a lot of attention in bioinorganic, medicinal chemistry, and supramolecular medicinal chemistry because they connect the structural motifs required for various biological activities and metal ion coordination through sulfonylamido, phenylamino groups, or donor atoms in substituents. After the introduction of organic drugs, metal ion complexes have drawn the increasing attention of researchers. The discovery and clinical application of the first metal ion complex – cisplatin [14] directed research in inorganic chemistry to the search for new chemotherapeutic agents. Since then, the investigation for new anticancer drugs based on metal ions has been largely focused on platinum. It led to the development of carboplatin [15] and oxaliplatin [16]. Cisplatin and its analogues are used in the treatment of many types of cancer, including ovarian [17], myelomas [18], melanoma [19], bladder [20], testicular [21], lung [22] as well as lymphomas [23]. However, its use has been associated with many undesirable side effects, including nephrotoxicity [24], and neurotoxicity [25]. It prompted to search for novel non-platinum chemotherapeutics which might exhibit cytostatic activity and could also be effective in cell resistance. The large variety of metal ions, types of ligands, and geometries make metal ion complexes suitable for the design of new drugs [26]. They show more favorable properties compared with organic molecules, in this case ligands themselves. The most important of them are the variable oxidation states and distinctive geometry of the metal ion complexes, which results in high structural diversity and participation in various biological redox reactions. Based on the success of platinum group metal ion complexes as anticancer agents, there has been increased interest in using metal ion complexes also as antimicrobial agents [27]. Recently, iridium, ruthenium, and rhodium complexes have gained growing popularity due to their high water solubility, relative accessibility, and easy synthesis [28]. Rhodium complexes have been shown as promising anticancer

* Corresponding author.
E-mail address: malgorzata.gawronska@ug.edu.pl (M. Gawrońska).

https://doi.org/10.1016/j.poly.2022.115865
Received 4 March 2022; Accepted 24 April 2022
Available online 27 April 2022

drugs since they exhibit slow ligand exchange kinetics, which is comparable to the time of cell division processes, so they are active in cancer cell apoptosis [29,30]. A large variety of rhodium ions complexes have found application in biological studies on anticancer [31] antibacterial [32], antifungal [33], antiviral [34], and anti-inflammatory [35] activity. Although medicine is making significant progress, more research into new drugs is needed. This necessity results from the very rapid progress of civilization diseases related to lifestyle and environmental changes. One of the most important preliminary parameters in the design of new drugs is the acid dissociation constant. Its value can provide information on drug properties such as lipophilicity, acidity, solubility, and permeability. Another parameter that is determined in the design of matallodrugs is the stability constant of complexes. These values are very important in many fields of science, such as biology, medicine, or chemistry and allow for quantitative calculations of the concentration of the formed complexes and their components.

In this paper, we reported the synthesis and structural studies of two new sulfonamide derivatives with hydroxyphenyl moiety, namely 4-amino-*N*-(2-hydroxyphenyl)benzenesulfonamide, and 4-amino-*N*-(3-hydroxyphenyl) benzenesulfonamide. Compounds were characterized by mass spectrometry (MS), elemental analysis (CHNS), spectroscopic (FT-IR, ^{1}H NMR, ^{13}C NMR), crystallographic (SC-XRD), and thermal (TG) methods. Taking into account the current research and the promising biological activity of Rh(III), it was selected for the determination of the complex formation constants. We hope that the results of these studies will form the basis for the further design and preparation of rhodium ion complexes with sulfa-drugs as anticancer and antibacterial agents.

2. Experimental

2.1. Substrates and solvents

The precursors, *N*-acetylsulfanilyl chloride, 2-aminophenol, and 3-aminophenol, were procured from Sigma-Aldrich and used without purification. Anhydrous pyridine was purchased from Sigma-Aldrich, methanol, chloroform, $NaHCO_3$ from POCH. Doubly distilled water (Hydrolab-Reference purified) with a conductivity not exceeding 0.09

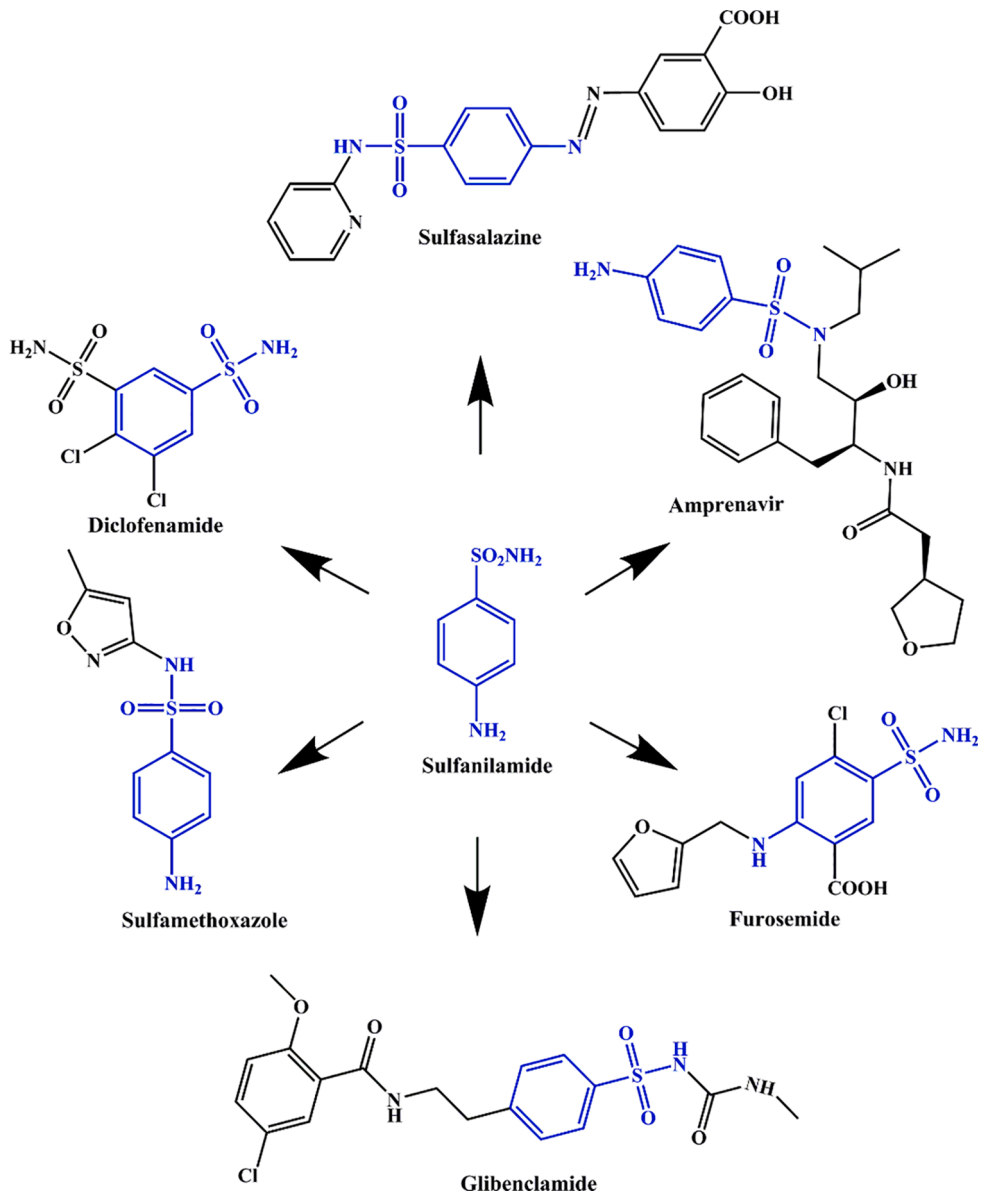

Fig. 1. Structure of sulfa drugs based on sulfanilamide scaffold – sulfamethoxazole [8]; furosemide [9]; glibenclamide [10]; diclofenamide [11]; amprenavir [12]; sulfasalazine [13].

μS/cm was used in the preparation of all the solutions. Additionally, stock solutions of HCl and KOH were prepared by dissolution of appropriate amounts of the compounds in double-distilled water. The hydrochloric acid stock solution was standardized by pH titration against Na_2CO_3. Sodium carbonate (from Sigma Aldrich) was calcined at 220 °C before the standardization of HCl.

2.2. Physicochemical methods

Mass spectra (MS) were obtained using a Bruker Daltonics (HCT Ultra) instrument. The infrared spectra were recorded on a Perkin Elmer Spectrum Two FT-IR spectrometer using an attenuated total reflectance (ATR) module with a diamond crystal in the spectral range of 4000 ÷ 400 cm^{-1}. The intensity of FT-IR bands was determined as s (strong), m (medium), and w (weak). The elemental analysis (CHNS) was recorded on an Elementar Vario El Cube analyzer. ^1H NMR and ^{13}C NMR spectra were acquired on Bruker AVANCE III spectrometer 500 and at 125 MHz, respectively. Chemical shifts were reported in δ (ppm) units using the residual solvent peaks as reference (DMSO-d_6 = 2.50 ppm). ^1H NMR coupling constants (*J*) were reported in Hertz (Hz), and multiplicity was indicated as follows: s (singlet), bs (broad singlet), d (doublet), dd (doublet of doublets), ddd (doublet of doublet of doublets), td (triplet of doublets), t (triplet). The thermogravimetric analysis (TGA) was carried out on a Perkin Elmer TGA 8000 thermogravimetric analyzer. The TG experiments were performed in an N_2 atmosphere at a heating rate of 10 °C/min in the temperature range of 30 ÷ 1100 °C using α-Al_2O_3 crucible. Analytical TLC was performed on aluminum sheets of silica gel UV-254 Merck and visualized with UV lamp at 254 nm. Melting points were determined on a Stuart melting point apparatus SMP3.

2.3. Synthesis

The synthesis of the sulfonamides **1** and **2** was carried out according to Scheme 1.

Synthesis of *N*-acetylsulfonamides – precursors for compound **1** and **2**.

2.3.1. *N-{4-[(2-hydroxyphenyl)sulfamoyl]phenyl}acetamide, N-{4-[(2-methoxyphenyl)sulfamoyl] phenyl}acetamide*

The 6.3 mmol of 4-acetamidobenzene-1-sulfonyl chloride was suspended in 10 cm^3 of anhydrous pyridine and appropriate aminophenol (6.0 mmol) [36]. The reaction mixture was heated at 60 °C for 4 h. The mixture was cooled to room temperature, poured into ice water, and acidified with 1 M HCl to pH 4. Completion of the reaction was monitored by thin-layer chromatography (TLC) on Silica Gel (Merck) in chloroform–methanol (v/v = 5:1) system solvent. The solid product was filtered, washed with water, and dried on air at room temperature. Compounds *N*-{4-[(2-hydroxyphenyl)sulfamoyl]phenyl}acetamide and *N*-{4-[(2-methoxyphenyl)sulfamoyl]phenyl}acetamide were obtained as brown solids with 50% and 54% yield, respectively.

2.3.2. *4-Amino-N-(2-hydroxyphenyl)benzenesulfonamide (1), 4-Amino-N-(3-hydroxyphenyl) benzenesulfonamide (2)*

N-{4-[(2-hydroxyphenyl)sulfamoyl]phenyl}acetamide and *N*-{4-[(2-methoxyphenyl) sulfamoyl]phenyl}acetamide (1 mmol) were dissolved in the 2 cm^3 of ethanol and the 1 cm^3 of concentrated HCl was added. The reaction mixture was stirred at 70 °C overnight, next diluted with water and basified with $NaHCO_3$ to pH 8. The solution was evaporated, and the residue was purified by column chromatography (Silica gel, Merck) in the solvent system: chloroform–methanol 50:1; 40:1; 30:1; 20:1; 10:1; 5:1: 2:1, respectively. Compounds **1** and **2** were obtained with 43% and 40% yield, respectively. The compounds were purified by recrystallization from methanol solution to obtain monocrystals suitable for X-ray study. The structures were checked and confirmed by mass spectrometry (MS), spectroscopic (FT-IR, ^1H NMR, ^{13}C NMR), and elemental analysis (CHNS). All spectra are included in the supplementary materials (Fig. S1 – S4). The structure of the obtained compound is shown in Scheme 2.

4-Amino-N-(2-hydroxyphenyl)benzenesulfonamide (**1**) – Yield: 54.0%. Mp.: 171–173 °C. Anal. Calcd. (%) for $C_{12}H_{12}N_2O_3S$ (264.30): C, 54.53; H, 4.58; N, 10.60; S, 12.13; Found (%): C, 54.11; H, 5.59; N, 10.68; S, 12.28; ESI-MS *m/z*: 263.1 [M−H]; FT-IR ATR (cm^{-1}): 3502 (w); 3401 (m); 3339 (w); 3245 (m); 2825 (w); 1902 (w); 1621 (m); 1596 (m); 1504 (m); 1470 (m); 1436 (w); 1410 (m); 1356 (w); 1328 (m); 1298 (m); 1277 (m); 1241 (m); 1188 (w); 1133(s); 1080 (s); 1038 (m); 1005 (w); 963

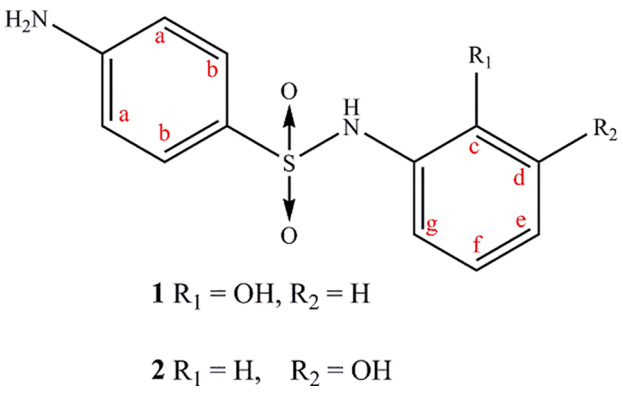

Scheme 2. Scheme of synthesized sulfonamides **1** and **2**. The scheme shown labels of appropriate protons.

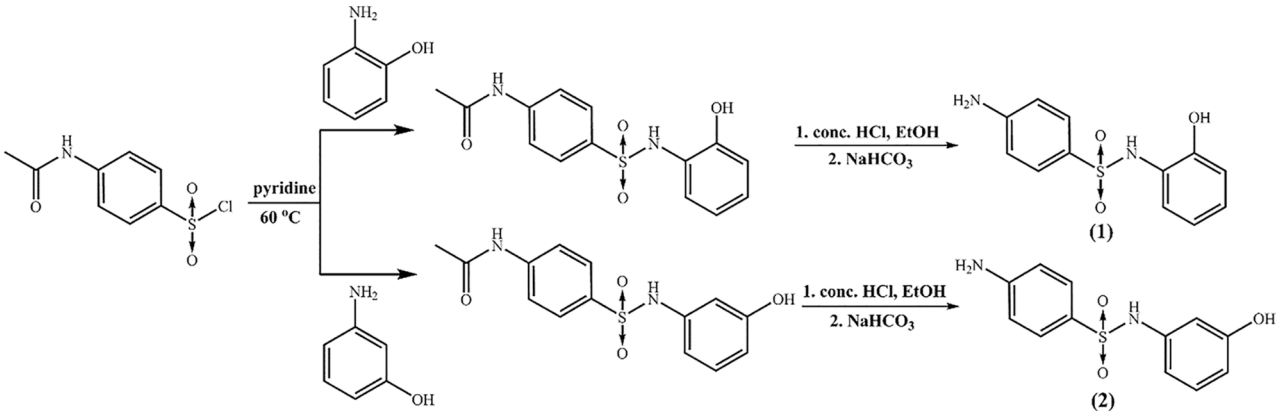

Scheme 1. Synthetic route of sulfonamides **1** and **2**. The first step contains sulfonamide bond formation between 4-acetamidobenzene-1-sulfonyl chloride and appropriate aminophenol in anhydrous pyridine. In the next step acetyl protection is removed in concentration HCl.

(w); 935 (m); 914 (m); 858 (w); 807 (m); 746 (s); 718 (m); 686 (s); 646 (s); 629 (m); 612 (m); 565 (s); 540 (s); 521 (s); 459 (m); 414 (m); ^{1}H NMR (DMSO-d_6) δ 5.91 (s, 2H, –N**H**$_2$); 6.51 (d, 2Ha, $J_{Ha:Hb}$ = 8.76 Hz); 6.68 (td, 1Hf, $J_{Hf:He,Hg}$ = 1.44 Hz; $J_{Hf:Hd}$ = 7.78 Hz); 6.73 (dd, 1Hd, $J_{Hd:Hf}$ = 1.44; Hz; $J_{Hd:He}$ = 8.50 Hz); 6.88 (td, 1He, $J_{He:Hg}$ = 1.59 Hz; $J_{He:Hd,Hf}$ = 7.76 Hz); 7.13 (dd, 1Hg, $J_{Hg:He}$ = 1.59; Hz; $J_{Hg:Hf}$ = 8.02 Hz); 7.37 (d, 1 Hb, $J_{Hb:Ha}$ = 8.71 Hz); 9.02 (bs, 2H, –SO$_2$N**H**; –O**H**); ^{13}C NMR (DMSO-d_6) δ 112.87; 115.84; 119.39; 123.49; 125.48; 125.63; 125.73; 129.20; 149.80; 153.14 ppm.

4-Amino-N-(3-hydroxyphenyl)benzenesulfonamide (**2**) – Yield: 32.0%. Mp.: 188–190 °C. Anal. Calcd. (%) for $C_{12}H_{12}N_2O_3S$ (264.30): C, 54.33; H, 4.58; N, 10.60; S, 12.13; Found (%): C, 54.12; H, 4.58; N, 10.54; S, 11.93; ESI-MS *m/z*: 262.9 [M−H]; FT-IR ATR (cm^{-1}): 3496 (w), 3383 (m), 3230 (m), 2665 (w), 1903 (w), 1629 (m), 1597 (s), 1569 (w), 1499 (m), 1466 (m), 1437 (w), 1397 (w), 1329 (m), 1295 (s), 1264 (m), 1207 (w), 1172 (m), 1139 (s), 1090 (s), 1076 (m), 1001 (w), 975 (m), 907 (m), 876 (w); 856 (w); 827 (m); 786 (w); 760 (m); 690 (s); 645 (m); 612 (m), 569 (s), 539 (s), 505 (m), 477 (m); 456 (m); 435 (m); ^{1}H NMR (DMSO-d_6) δ 5.94 (s, 2H, –N**H**$_2$); 6.36 (ddd, 1Hg, $J_{Hg:He}$ = 0.90 Hz, $J_{Hg:Hc}$ = 2.26 Hz, $J_{Hg:Hf}$ = 8.14 Hz); 6.49 (ddd, 1He, $J_{He:Hg}$ = 0.86 Hz, $J_{He:Hc}$ = 2.06 Hz, $J_{He:Hf}$ = 8.03 Hz); 6.54 (d, 1Ha, $J_{Ha:Hb}$ = 8.84 Hz); 6.56 (t, 1Hc, $J_{Hc:He,Hg}$ = 2.14 Hz); 6.95 (t, 1Hf, $J_{Hf:He,Hg}$ = 8.04 Hz); 7.39 (d, 1Hb, $J_{Hb:Ha}$ = 8.73 Hz); 9.34 (s, 1H, –O**H**); 9.72 (s, 1H, –SO$_2$N**H**) ^{13}C NMR (DMSO-d_6) δ 106.80; 110.45; 110.81; 113.00; 125.11; 129.13; 130.01; 140.03; 153.23; 158.19 ppm.

2.4. Crystal structure determination

Single crystal X-ray diffraction data of compounds **1** and **2** were collected at 120(2) K on a Stoe IPDS-2 T diffractometer with graphite monochromated Mo-Kα radiation. Data collection and image processing were performed with X-Area 1.75 (STOE and Cie GmbH, Darmstadt, Germany, 2015) [37]. Intensity data were scaled with LANA (part of X-Area) to minimize differences in intensities of symmetry-equivalent reflections (multi-scan method). The crystal was thermostated in a nitrogen stream at 120 K using CryoStream-800 device (Oxford CryoSystem, Long Hanborough OX29, UK) during the entire experiment. Because of the low absorption of X-rays by the crystals, no absorption corrections were applied. The structures of **1** and **2** were solved with the ShelXT [38] structure solution programs run under Olex2 [39] using Intrinsic Phasing and refined with the ShelXL [40] refinement package. The WinGX [41] program was used to prepare the final version of the CIF files. Diamond [42] was used to prepare the figures. All non-hydrogen atoms were refined anisotropically. Positions of the hydrogen atoms were calculated geometrically and taken into account with isotropic temperature factors. Positions of the N—H and O—H hydrogen atoms were found in the electron density Fourier map and refined without constraints, except for N2′–H, where these atoms were refined as riding atoms with N—H = 0.88 Å with U_{iso} = 1.2 U_{eq}(C). One phenyl ring and an amine group in **2** have been modeled as disordered: C1′–C6′ and N2′ (*s.o.f.* of 0.631(2) and 0.369(2)). Displacement ellipsoids of the carbon and nitrogen atoms tend to achieve very high values so EADP SHELX instruction was applied to constrain them. A summary of crystallographic data is shown in Table 1.

2.5. Spectrophotometric determination of pKa values

All UV–Vis measurements were carried out at room temperature using Thermo Scientific Evolution 300 spectrophotometer equipped with an automatic microtitrator (Cerko). To determine acid-base properties of sulfonamide derivatives 2 cm^3 of investigated samples (concentration in the range of $1.4{\cdot}10^{-5} \div 2.0{\cdot}10^{-5}$ M) dissolved in $5.27{\cdot}10^{-3}$ M HCl aqueous solution were titrated by $2.09{\cdot}10^{-2}$ M KOH, previously degassed with Ar. The electronic spectra were registered in a wavelength range of 200 ÷ 400 nm and the dissociation constants (pK_a) have been calculated based on the modified Henderson-Hasselbalch equation (1):

Table 1
Crystallographic data and structure refinement details for compounds **1** and **2**.

Empirical formula	$C_{12}H_{12}N_2O_3S$ (**1**)	$C_{12}H_{12}N_2O_3S$ (**2**)
Formula weight (g mol^{-1})	264.30	264.30
Temperature (K)	120(2)	120(2)
Wavelength (Å)	0.71073 (Mo K$_\alpha$)	0.71073 (Mo K$_\alpha$)
Crystal system	monoclinic	monoclinic
Space group	$P2_1/n$	$P2_1/c$
Unit cell dimensions		
a (Å)	9.3609(9)	18.7377(13)
b (Å)	13.0505(9)	17.4077(8)
c (Å)	9.8622(8)	7.2908(5)
β (°)	101.244(7)	90.545(5)
Volume (Å^3)	1181.68(17)	2378.0(3)
Z	4	8
Calculated density (Mg m^{-3})	1.486	1.476
Absorption coefficient (mm^{-1})	0.276	0.274
F(000)	552	1104
Crystal size (mm)	0.31 × 0.26 × 0.18	0.28 × 0.20 × 0.17
Theta range for data collection (°)	2.621–29.214	2.580–29.214
Limiting indices	$-12 \le h \le 12$, $-17 \le k \le 17$, $-13 \le l \le 13$	$-25 \le h \le 25$, $-23 \le k \le 23$, $-9 \le l \le 9$
Reflections collected / unique [I > 2sigma(I)]	14018 / 3176 [R_{int} = 0.0272]	27379 / 6359 [R_{int} = 0.0173]
Completeness to Θ_{max} (%)	99.6	99.5
Refinement method	Full-matrix least-squares on F^2	Full-matrix least-squares on F^2
Data / restraints / parameters	3176 / 0 / 179	6359 / 0 / 385
Goodness-of-fit on F^2	1.087	1.066
Final R indices [I > 2sigma (I)]	R_1 = 0.0370, wR_2 = 0.1016	R_1 = 0.0464, wR_2 = 0.1163
R indices (all data)	R_1 = 0.0387, wR_2 = 0.1028	R_1 = 0.0495, wR_2 = 0.1188
Largest diff. peak and hole (e Å^{-3})	0.745 and −0.487	0.634 and −0.565
CCDC deposition number	2130151	2129928

$$A = \frac{A_1 + A_2 \bullet 10^{(pH-pK_{a1})}}{10^{(pH-pK_{a1})} + 1} + \frac{A_2 + A_3 \bullet 10^{(pH-pK_{a2})}}{10^{(pH-pK_{a2})} + 1} + \frac{A_3 + A_4 \bullet 10^{(pH-pK_{a3})}}{10^{(pH-pK_{a3})} + 1} \quad (1)$$

where A_n is absorbance of various protonated forms.

2.6. Spectrophotometric determination of complex formation constants

The solutions of the compounds studied and Rh(III) salt were prepared in water directly before measurements and maintained at a constant temperature of 25 °C. The concentrations of examined ligands measured spectrophotometrically were $5.41{\cdot}10^{-4}$ M for **1** and $2.89{\cdot}10^{-4}$ M for **2** systems studied. The concentration of metal ion was about 10 times higher than ligands **1** and **2**, $5.78{\cdot}10^{-5}$ M and $3.03{\cdot}10^{-5}$ M, respectively.

The spectrophotometric titrations were performed by adding to the solution of appropriate ligand a solution of metal salt dissolved in the ligand. These titrations were performed with a constant concentration of the additive. In this measurement, Rh(III) chloride tetrahydrate, $RhCl_3{\cdot}4H_2O$, was used. The complex formation between investigated sulfonamide derivatives and Rh(III) ion was monitored by UV–Vis titration (wavelength range of 210 ÷ 800 nm) of ligand samples dissolved in methanol by the mixture of the same ligand solution and $RhCl_3$. During titration constant concentration of a ligand has been preserved to observe only changes related to the interaction of metal ion and sulfonamide derivatives. All solutions were prepared immediately before the studies. To guarantee reproducibility of the obtained results measurements were repeated in independent series.

Stability constants of rhodium(III)-**1** or **2** complexes were determined using the EQUID program [43] by a minimization of the

differences between the experimental data and theoretical model (the non-linear least-squares Gauss-Newton-Marquardt algorithm for a fitting procedure). Interestingly, both of the sulfa ligands (H_2L) are presented in their anionic forms $(HL^n)^-$ due to the methanolic medium used in the experiments. The gradual K and cumulative β stability constants can be described by the following equation (2) where (n) denotes the type of ligand **1** or **2**:

$$\left[Rh(OH_2)_4\right]^{3+} + (HL^n)^- \leftrightarrows \left[Rh(OH_2)_4HL^n\right]^{2+}$$

$$\beta = K_1 = \frac{\left\{\left[Rh(OH_2)_4\ HL^n\right]^{2+}\right\}}{\left\{\left[Rh(OH_2)_4\right]^{3+}\right\}\cdot[(HL^n)^-]} \quad (2)$$

3. Results and discussion

3.1. Synthesis and spectroscopy

Two sulfonamides *4-Amino-N-(2-hydroxyphenyl)benzenesulfonamide* (**1**), and *4-Amino-N-(3-hydroxyphenyl) benzenesulfonamide* (**2**) have been synthesized. The structures of obtained compounds were checked by mass spectrometry (MS), elemental analysis (CHNS), spectroscopic (FT-IR, ^{1}H NMR, ^{13}C NMR), crystallographic (SC-XRD), and thermal (TG) methods. The ^{1}H NMR spectra (Fig. S1a and S1b) of **1** and **2** showed signals assigned to aromatic protons of both sulfonamide derivatives in the region between 6.36 and 7.37 ppm. The spectra also showed a singlet peak at 9.72 ppm for **2** derived from protons of the sulfonamide group –SO_2NH–. The presence of hydroxyl –OH protons was observed as a singlet peak at 9.34 ppm for **2**. The proton of the amine –NH_2 group manifests its presence as a singlet peak at 5.91 and 5.94 ppm of **1** and **2**, respectively. The aromatic carbon atoms of both derivatives showed signals in the region between 106.84 and 158.24 ppm in ^{13}C NMR spectra (Fig. S2a and S2b).

The FT-IR spectra of compounds **1** and **2** contain characteristic bands of the vibrations of sulfonamide group –SO_2NH–, amine group –NH_2, and hydroxyl group –OH (Fig. S3a and S3b). The stretching ν(O—H) vibrations are visible as broad bands at 3502 and 3496 cm^{-1} for **1** and **2**, respectively. Two medium-intensity bands in the range of 3401 ÷ 3230 cm^{-1} are assigned to the N—H stretching vibrations and single bands in the range of 1629 ÷ 1640 cm^{-1} are assigned to the N—H bending vibrations of primary aromatic amine. The ν(N—H) vibrations in sulfonamide groups appear in the region 3339 ÷ 3230 cm^{-1}. The bands of –SO_2– asymmetric and symmetric stretching vibrations are located in the range of 1328 ÷ 1397 cm^{-1} and 1132 ÷ 1139 cm^{-1}, respectively. The stretching vibrations bands of aromatic rings ν(C═C) come in the region of 1591 ÷ 1499 cm^{-1}. The stretching ν(S—N) vibrations are assigned in the region 684 ÷ 689 cm^{-1}.

3.2. Thermogravimetric analysis

The thermal behavior of compounds **1** and **2** was evaluated by thermogravimetric analysis (TGA). The TG curves are given in Fig. 2. The first small loss of weight observed on the TG curve of **1** takes place over 120 °C (<1.5%) and can be caused by the presence of residue solvent molecules or moisture. The essential thermal decomposition begins at over 220 °C for **1** and over 190 °C for **2**. The DTG curves in those temperatures revealed single peaks with peak temperatures of 302.3 °C and 263.3 °C corresponding to the maximum speed of the decomposition of **1** and **2**, respectively. The highest thermal decomposition rate slows down at about 340 °C. The final degradation step is characterized by the lower weight loss rate with one distinct maximum at 631.8 °C on DTG curve of **1** and two partially separated maxima at 626.1 and 713.8 °C on DTG curve of **2**. The TG curves reach the weight values near to zero at about 700 and 800 °C for **1** and **2**, respectively. A very small ashy residue is completely decomposed at about 1000 °C.

3.3. Crystal structure and conformational analysis

The results of the X-ray diffraction experiments are presented in Table 1. 4-Amino-*N*-(2-hydroxyphenyl)benzenesulfonamide (**1**) crystallizes in the monoclinic space group $P2_1/n$ with the one molecule (*A*) per asymmetric unit, while 4-amino-*N*-(3-hydroxyphenyl)benzenesulfonamide (**2**) crystallizes in the $P2_1/c$ space group with the two independent molecules (*A* and *B*) per asymmetric unit. The molecular structures of sulfonamides **1** and **2** are shown in Fig. 3 and the bond lengths and angles are shown in Table S1 (Supplementary materials). In the presented sulfonamide molecules the S1(*A*) and S1′(*B*) atoms are connected through C1(*A*) and C1′(*B*) atoms with phenyl ring substituted in the 4-position by an amine group. The *N*-site of the molecules consists of the *o*-hydroxyphenyl group in **1** and the *m*-hydroxyphenyl group in **2** connected with N2 (N2′) atom.

In the description of the coordination polyhedra around S-atom of sulfonamide group, Okuniewski's τ'_4 structural parameter was used [44,45] (eq. (3)):

$$\tau'_4 = \frac{\beta - \alpha}{360^\circ - \theta} + \frac{180^\circ - \beta}{180^\circ - \theta} \quad (3)$$

where $\beta > \alpha$ are two greatest valence angles and $\theta = \cos^{-1}(-1/3) \approx 109.5^\circ$ is the tetrahedral angle. For square planar geometry $\tau'_4 = 0$ and for tetrahedral geometry $\tau'_4 = 1$. The atoms around the sulfonamide S-atoms are arranged in a slightly distorted tetrahedral geometry, with

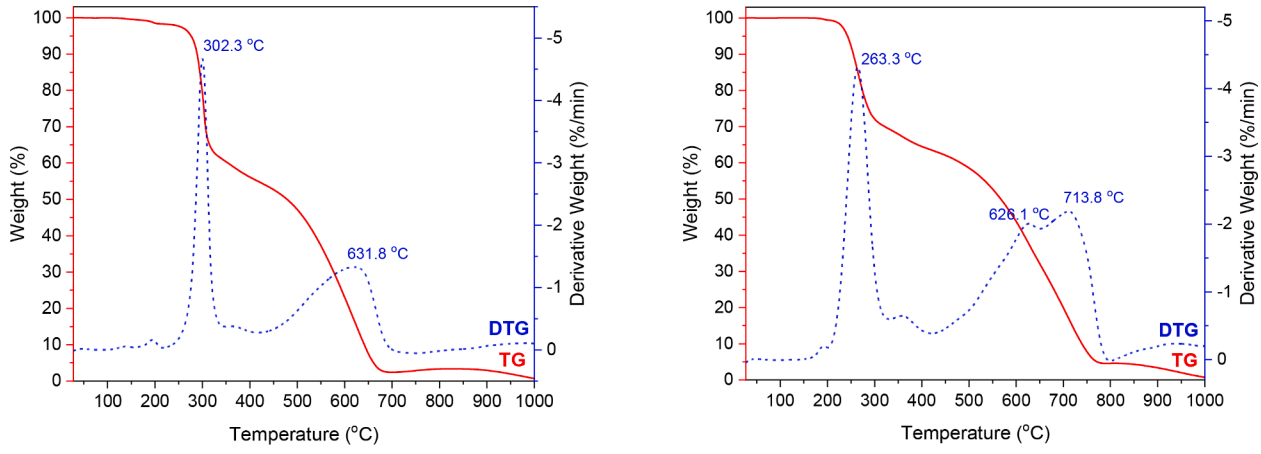

Fig. 2. TG/DTG curves of the thermal decomposition of sulfonamides (a) **1**; (b) **2**.

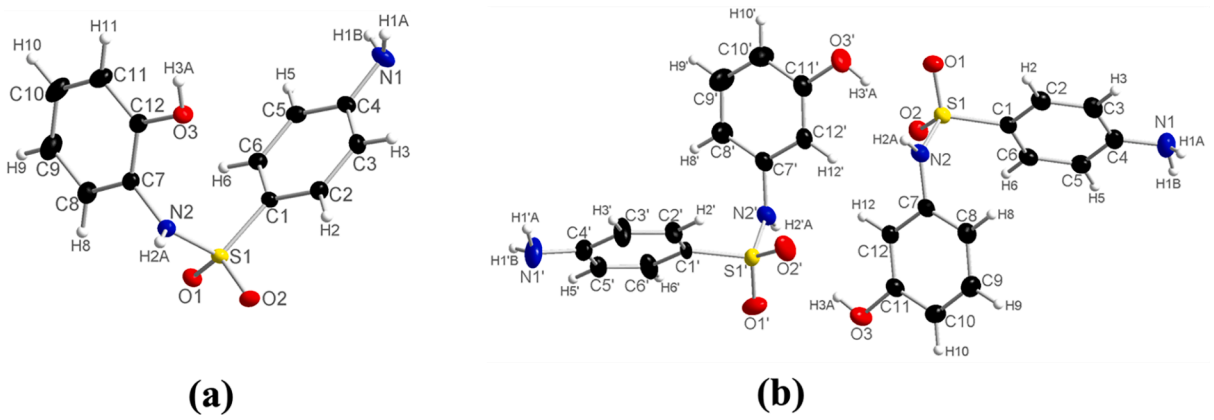

Fig. 3. Asymmetric units of (a) **1** and (b) **2** compounds show labelling. The displacement ellipsoids are drawn at the 50% probability level.

$\tau'_4 = 0.91$ (S1) and $\tau'_4 = 0.90$ (S1′).

The conformational states of the mentioned sulfonamide molecules depend on the mobility of the bridge, connecting two phenyl rings: Ph1 (C1–C6) and Ph2 (C7–C12). In order to describe the conformational state of the molecules, the following four parameters have been chosen: the torsion angle between the $–SO_2–$ group and the phenyl ring Ph1 < C—C—S—N (τ_1); the torsion angle <C—S—N—C (τ_2), which describes the mobility of the S—N bond; the torsion angle <S—N—C—C (τ_3), which characterizes the location of the second phenyl ring Ph2 concerning the –NH– group and the angle between the two phenyl rings <Ph1–Ph2 (the acute angle between the least-squares planes through the two phenyl rings). The results are summarized in Table 2. All the molecules are V-shaped with the sulfonamide S1 (S1′) atom at the apex of each V. The dihedral angles between two phenyl rings are in the range of 47.9 ÷ 65.7° and are in accordance with previous studies [46,47]. The torsion angles take positive values in the molecule of ortho-hydroxysulfonamide **1**, which indicate a (+)-synclinal conformation. The two molecules of **2** (*A* and *B*) are twisted in opposite directions, since the torsions angles take negative and positive values in *A* and *B*, respectively. Consequently, molecule **2**(*A*) adopts (–)-synclinal and **2**(*B*) (+)-synclinal conformation in the solid-state [36].

The crystal packing results especially from the combination of H-bonds. In the structures of hydroxyphenylsulfonamides **1** and **2** here are O—H donors derived from the hydroxyphenyl moiety and N—H donors from both sulfonamide and amine groups. The H-accepting abilities are observed mainly in O-sulfonyl and O-hydroxy acceptors. The hydrogen bonds parameters for **1** and **2** are listed in Table 3. In the crystal structure of **1** molecules are self-assembled into centrosymmetric dimers

Table 3
Selected X-ray geometrical parameters of H-bonds in sulfonamides **1** and **2**. Distances are in angstroms (Å), and angles in degrees (°). The labels correspond to those from Fig. 4.

D–H···A	D–H (Å)	H···A (Å)	D···A (Å)	D–H···A (°)	Graph-set motif
1					
O3–H3A···O1^{i}	0.84	1.919(1)	2.746(2)	167.7	C(7)
N2–H2A···O2^{ii}	0.88	2.236(0)	2.945(2)	137.4	$R_2^2(8)$
N1–H1A···O2^{iii}	0.88	2.797(5)	3.052(5)	98.3	C(8)
N1–H1B···O2^{iii}	0.88	2.785(0)	3.404(8)	128.3	C(8)
2					
O3–H3A···O2′	0.84	2.028(5)	2.866(7)	176.0	$R_2^2(16)$
O3′–H3′A···O2	0.84	2.018(5)	2.848(7)	169.4	
N2–H2A···O1^{i}	0.88	2.427(2)	2.971(0)	120.5	C(4)
N2′–H2′A···O1^{ii}	0.88	2.216(2)	2.913(0)	136.0	C(4)
N1–H1A···O3^{iii}	0.90	2.722(0)	3.096(1)	106.0	C(12)
N1–H1B···O2′^{iv}	0.90	2.780(4)	3.449(5)	132.1	D
N1′–H1′A···O3′^{v}	0.88	2.663(4)	3.157(5)	116.6	C(12)
N1′–H1′B···O3′^{vi}	0.88	2.729(0)	3.322(2)	125.9	C(12)

Symmetry codes: Compound **1**: (i) 1.5-x,-0.5 + y,1.5-z; (ii) 1-x,1-y,1-z; (iii) 1 + x,y,z; Compound **2**: (i) x,0.5-y,-0.5 + z; (ii) x,1.5-y,0.5 + z; (iii) 1-x,-0.5 + y,0.5-z; (iv) 1-x,1-y,1-z; (v) -x,1-y,1-z; (vi) -x,0.5 + y,1.5-z.

Table 2
Selected X-ray geometrical parameters describing molecular conformational states in the crystal lattices of sulfonamides **1** and **2**. The angle values are in degrees (°).

Geometrical parameter	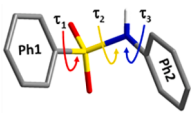	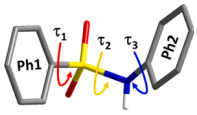	
	Angle (°)		
	1	**2(*A*)**	**2(*B*)**
τ_1 (C—C—S—N)	93.0	−80.3	71.6
τ_2 (C—S—N—C)	59.2	−60.3	61.4
τ_3 (S—N—C—C)	75.5	−83.8	79.5
<Ph1–Ph2	47.9	50.0	65.7
Conformation	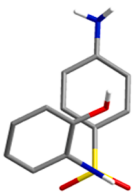 (+)-Synclinal	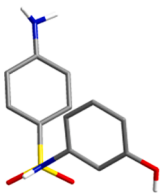 (−)-Synclinal	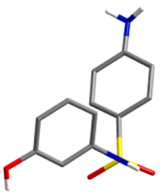 (+)-Synclinal

through pairwise N2–H2A···O2^{ii} hydrogen bonds formed between sulfonamide N—H donor group of the first molecule and sulfonamide O-acceptor of the second molecule at the distance of d(H···O) = 2.236 Å (Fig. 4a). According to Bernstein [48] these interactions represent an $R_2^2(8)$ ring graph-set motif. The dimers are further connected *via* O3–H3A$_{hydroxy}$···O1$^{i}_{sulfonamide}$ hydrogen bonds in *bc* plane at the H···O distance of 1.919 Å. These interactions form *zig-zag* chains along *b* axis with a simple C(7) chain motif. Such formed 2D net is extended into *a* direction through N—H(amine)···O(sulfonamide) weak hydrogen bonds at the H···O distance above 2.7 Å, generating a 3D network. In the crystal structure of **2** molecules A and B interact with each other *via* O3–H3A$_{hydroxy}$···O2′$_{sulfonamide}$ and O3′–H3′A$_{hydroxy}$···O2$_{sulfonamide}$ hydrogen bonds forming dimeric units with $R_2^2(16)$ graph-set motif [48]. The dimers are further connected *via* N2(N2′)–H2A(H2′A)···O1^{i}(O1′^{ii}) hydrogen bonds characterized by C(4) chain motif (Fig. 4b). These H-bonds forms a 2D network in the *bc* plane, which is extended in the *a* direction by the combination of rather weak N—H···O interactions between amine NH_2-donors and hydroxy or sulfonamide O-acceptors

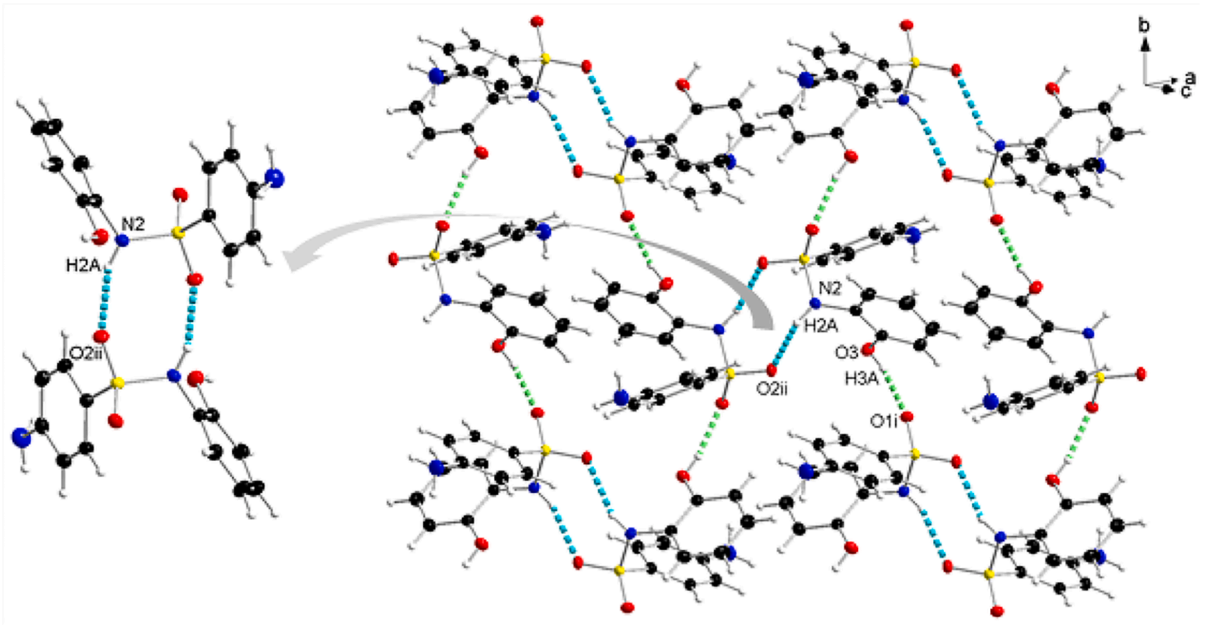

(a)

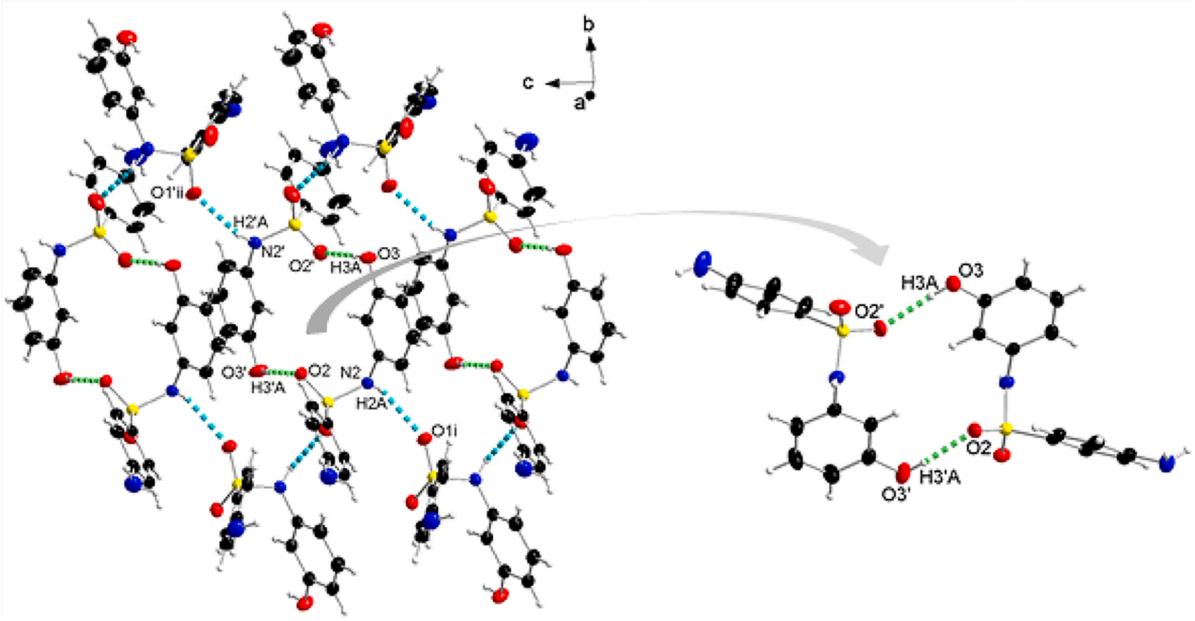

(b)

Fig. 4. Geometry of N—H···O and O—H···O hydrogen bonds in the crystal structures of sulfonamides (a) **1** and (b) **2**. (Symmerty codes for **1**: (i) 1.5-x,-0.5 + y,1.5-z; (ii) 1-x,1-y,1-z; for **2**: (i) x,0.5-y,-0.5 + z; (ii) x,1.5-y,0.5 + z).

(Table 3).

3.4. Acid-base properties

Acid-base properties are of the most important ones in terms of organic compounds' reactivity and their further design as potential drugs. Indeed, knowledge of the acid dissociation constant allows us to control the ionization state of substances which affects their solubility and lipophilicity as well as distribution and metabolism in biological systems [49,50]. To determine acid-base properties of the synthesized sulfonamide derivatives the UV spectrophotometric titration has been applied. Such a technique offers high precision and sensitivity while studying chemical equilibria occurring in solutions for compounds with lower solubility. The results of electronic absorption titration for both compounds **1** and **2** are presented in Fig. 5.

Comparison of UV spectra of acidified sample **1** (Fig. 5a) indicates hyperchromic and hypsochromic shifts of the maximum at 267 nm as well as the gradual appearance of the band at 295 nm associated with increasing pH from 3.0 to 11.3. To make the interpretation of spectrophotometric results easier, absorption spectra obtained in the most acidic, neutral, and extremely basic solutions have been marked with red, blue, and green colors, respectively. Similar changes can be observed during titration of the initially protonated **2** (Fig. 5b, pH range of 2.8 ÷ 11.2). Such variations in absorbance, together with isosbestic points, confirm equilibria occurring in the solutions of samples **1** and **2** under experimental conditions. To obtain the exact number of equilibria A-diagrams were plotted (**1**: A at 277 nm *vs.* A at 206 nm, **2**: A at 252 nm *vs.* A at 226 nm) and shown in Fig. 5b,e. For both **1** and **2**, three regions with the linear dependence between absorbance can be distinguished. It points to the existence of three dissociation reactions in the tested aqueous solutions, *i.e.* analyzed compounds occur in four species depending on the pH of the environment. The relationships of absorbance at 304 nm for **1** and 252 nm for **2** as a function of pH are given in Fig. 5c,f, where grey lines are fitted to experimental points (colored squares). Based on the Henderson-Hasselbalch equation the deprotonation constants together with standard deviations have been calculated and summarized in Table 4.

To determine the pK_a value, compounds **1** and **2** were dissolved in hydrochloric acid, hence they contain in their structures: primary ammonium group $–NH_3^+$, sulfonamide group $–SO_2NH–$ and hydroxyl group –OH which can dissociate protons under specific pH conditions. The proposed acid dissociation process of the analyzed compounds is illustrated in Scheme 3. The values of the calculated acid dissociation constants indicate that in the acidic solution compounds exist in the fully protonated forms. The first acidity constant (pK_{a1}) is associated with the equilibrium between the positively charged amine group of sulfonamide derivatives ($–NH_3^+$) and their electrically neutral conjugate bases. As the pH increases, the subsequent steps are related to deprotonation of amide (pK_{a2}) and hydroxyl (pK_{a3}) species which lead to the formation of dianions of molecules **1** and **2** in strongly basic solutions.

The reliability of the obtained pK_a values can be confirmed by comparison with literature data that indicate that acidity constants related to sulfonamides are usually in a range of 1.7 ÷ 2.4 (pK_{a1}) and

Table 4
Determined acidity constants with their standard deviations for compounds **1** and **2**. The values were obtained from the spectrophotometric titration measurements in aqueous solution at room temperature.

Compound	pK_{a1}	pK_{a2}	pK_{a3}
1	2.40 ± 0.20	5.96 ± 0.27	9.36 ± 0.01
2	2.35 ± 0.14	5.44 ± 0.05	9.56 ± 0.01

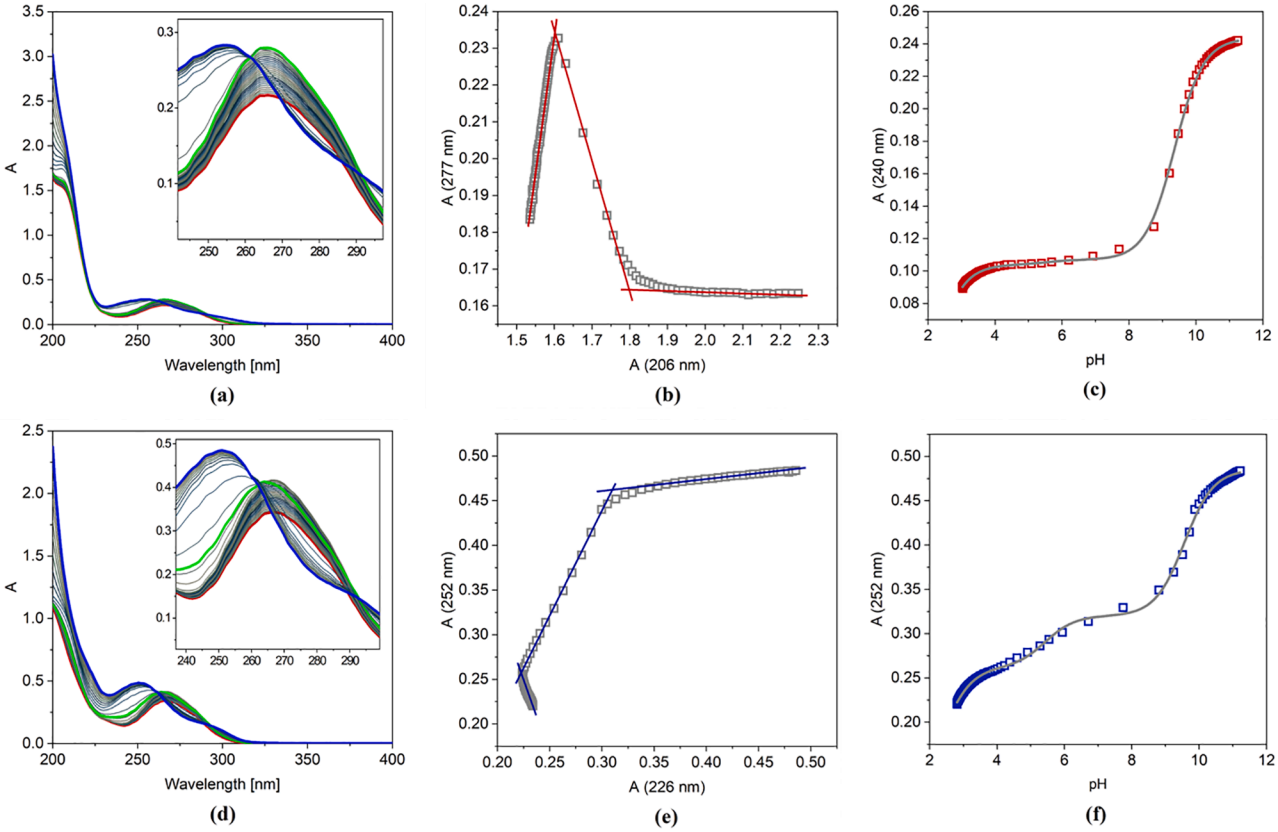

Fig. 5. The results of spectrophotometric acid-base titration of sulfonamides (a-c) **1** and (d-f) **2**. (a, d) UV spectral curves – pH < 3 red, pH ~ 7 green, pH > 11 blue; (b, e) representative A-diagrams; (c, f) absorbance at specific wavelength as a function of pH – red and blue squares represent experimental points whereas grey lines result from mathematical fitting.

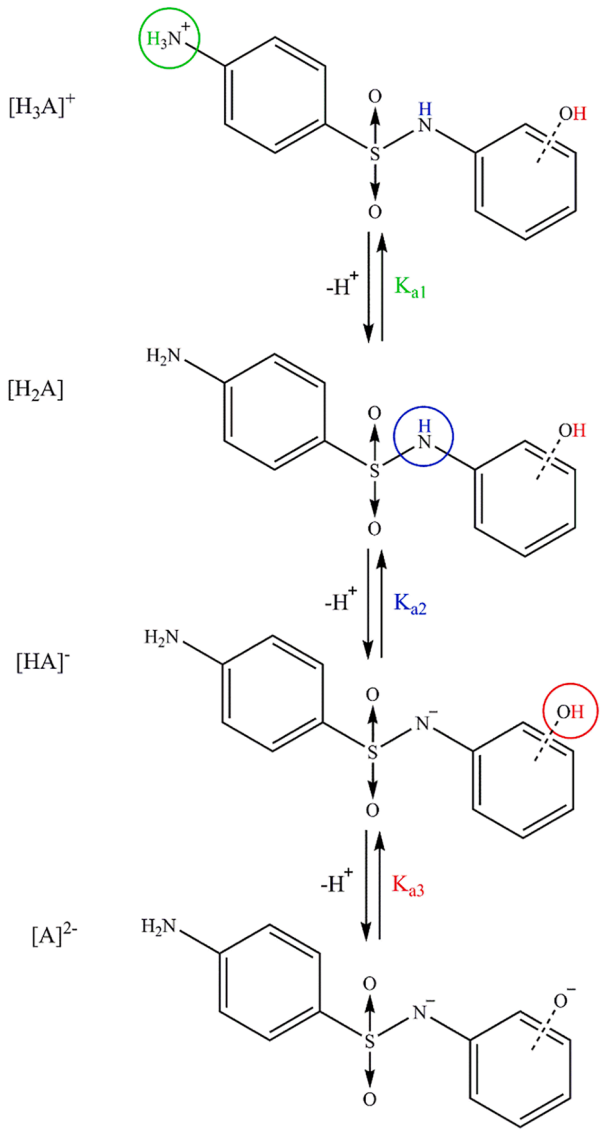

Scheme 3. Proposed deprotonation sites of sulfonamide derivatives **1** and **2**.

5.2 ÷ 6.8 (pK_{a2}) [51-53]. Furthermore, the deprotonation constant of phenolic hydroxyl group for similar organic structures as investigated **1** and **2** varies from 8.8 to 9.6 [54,55].

3.5. Rhodium(III) complex formation

The coordination chemistry of rhodium(III) has provided several interesting properties that enhance catalytic as well as biological activities of Rh(III) complexes [56,57]. The establishing coordination mode is an important study to elucidate the mechanism of action for metalloantibiotics and structural aspects of sulfa ligands binding sites used to stabilization of metal cations. All these considerations prompted the preparation of spectrophotometric titrations to determine the affinity of sulfonamide derivatives **1** and **2** for rhodium(III) ions. Indeed, UV–Vis spectra were recorded in an attempt to understand the modes mentioned. The electronic spectra of the uncoordinated ligands **1** and **2** are presented as black and bold-face line in Fig. 6 to show one band in the 210 ÷ 600 nm range, 276 nm for **1** and 268 nm for **2**. The change in the hydroxyl substituent position (*ortho* to *meta*) seems to lead to a slightly (8 nm) blue shift as a result of the destabilization of the π* orbitals. Upon complexation with Rh(III) ion, the intensity of the ligand-centered (LC) band increases with a slight shift in relation to the ligand, in both cases. Moreover, the spectra should exhibit, in addition to LC bands, also broad bands assigned to metal–ligand charge transfer (MLCT) transitions. These MLCT and d-d transitions are related to the colors of Rh(III) complexes. However, the very weak d-d transitions could not be observed in the presence of the strong and/or broad LC bands in such low concentrations of metal salt and ligands in solutions. Due to the above, the maxima registered helped to determine the stoichiometry and demonstrate that equilibrium takes place in both systems studied. Moreover, based on the analysis of the spectrophotometric titration curves, the number of equilibria and stoichiometry of formed Rh(III) complexes were determined (Fig. 6). The intensities of absorption bands increases and hyperchromic effects can be observed for both systems. This observation suggests the existence of metal ion interactions with hard *N*-donor atoms of sulfa ligands **1** and **2**.

In order to indicate the exact number of equilibria presented in the system studied, the A-diagrams were plotted. The dependences of the absorbance at 256 nm on the absorbance at 270 nm for Rh(III)-**1** system and at 286 nm on the absorbance at 256 nm for Rh(III)-**2** were obtained (see Fig. 6 inside a and c). One straight section presented in the plot confirmed one equilibrium during the complexation process in both cases. The dependence of absorbance at 256 nm for **1** and 245 nm for **2** as a function of molar ratio $n_{Rh(III)}/n_{1\ or\ 2}$ is presented in Fig. 6b and d. The fitted data confirmed 1:1 metal:ligand stoichiometry of the complex formation process for both rhodium(III)-sulfa complexes.

The proposed complexing equilibria models correspond to the formation of two Rh(III) ion-sulfa ligand complexes of the stoichiometry of 1:1 (metal:ligand). Only mononuclear species were found. Based on the results from spectrophotometric measurements the values of gradual and cumulative formation constants for Rh(III) complexes were determined (Table 5). Differences, in log units, between the β values obtained provide a one-step coordination reaction. The errors quoted are the standard deviations of the overall stability constants given directly by the program (Table 5).

Interestingly, the high cumulative constants values of Rh(III)-sulfa complexes obtained are in our opinion directly related to the ionic form of sulfa ligands present in the methanolic solutions. Moreover, in the case of derivative **1**, other, more stable structure can be proposed. Due to the proximity of the –OH group in the *ortho* position of the phenyl ring the formation of complex with 5-membered chelate ring and Rh(III) ionic centre is highly possible. The mentioned hydroxyl group position gives stabilization of Rh(III) by an additional O-donor atom in this ligand to show bidentate properties of **1**.

4. Conclusions

In this study, two sulfonamides: 4-amino-*N*-(2-hydroxyphenyl)benzenesulfonamide (**1**) and 4-amino-*N*-(3-hydroxyphenyl)benzenesulfonamide (**2**) have been synthesized. Both compounds were characterized by mass spectrometry (MS), elemental analysis (CHNS), spectroscopic (FT-IR, ^{1}H NMR, ^{13}C NMR), crystallographic (SC-XRD), and thermal (TG) methods, and the values of acid dissociation constants were determined. Compound **1** crystallizes in the $P2_1/n$ space group with the one molecule (*A*) per asymmetric unit, while compound **2** crystallizes in the $P2_1/c$ space group with the two independent molecules (*A* and *B*) per asymmetric unit. All the molecules are V-shaped with the sulfonamide S1 (S1′) atom at the apex of each V. The torsion angles bear positive values in compound **1**, which indicates a (+)-synclinal conformation. While two molecules of **2** (*A* and *B*) are twisted in opposite directions, since the torsions angles bear negative and positive values in *A* and *B*, respectively. It showed that molecule **2**(*A*) adopts (–)-synclinal and **2**(*B*) (+)-synclinal conformation in the solid state. The stability constants for the complexation of rhodium(III) ion with sulfonamide derivatives **1** and **2** were determined spectrophotometrically in methanol. The results obtained from experimental measurements allowed us to conclude that the examined complexes of Rh(III) are stable in methanolic solutions which is confirmed by the values of gradual and cumulative stability

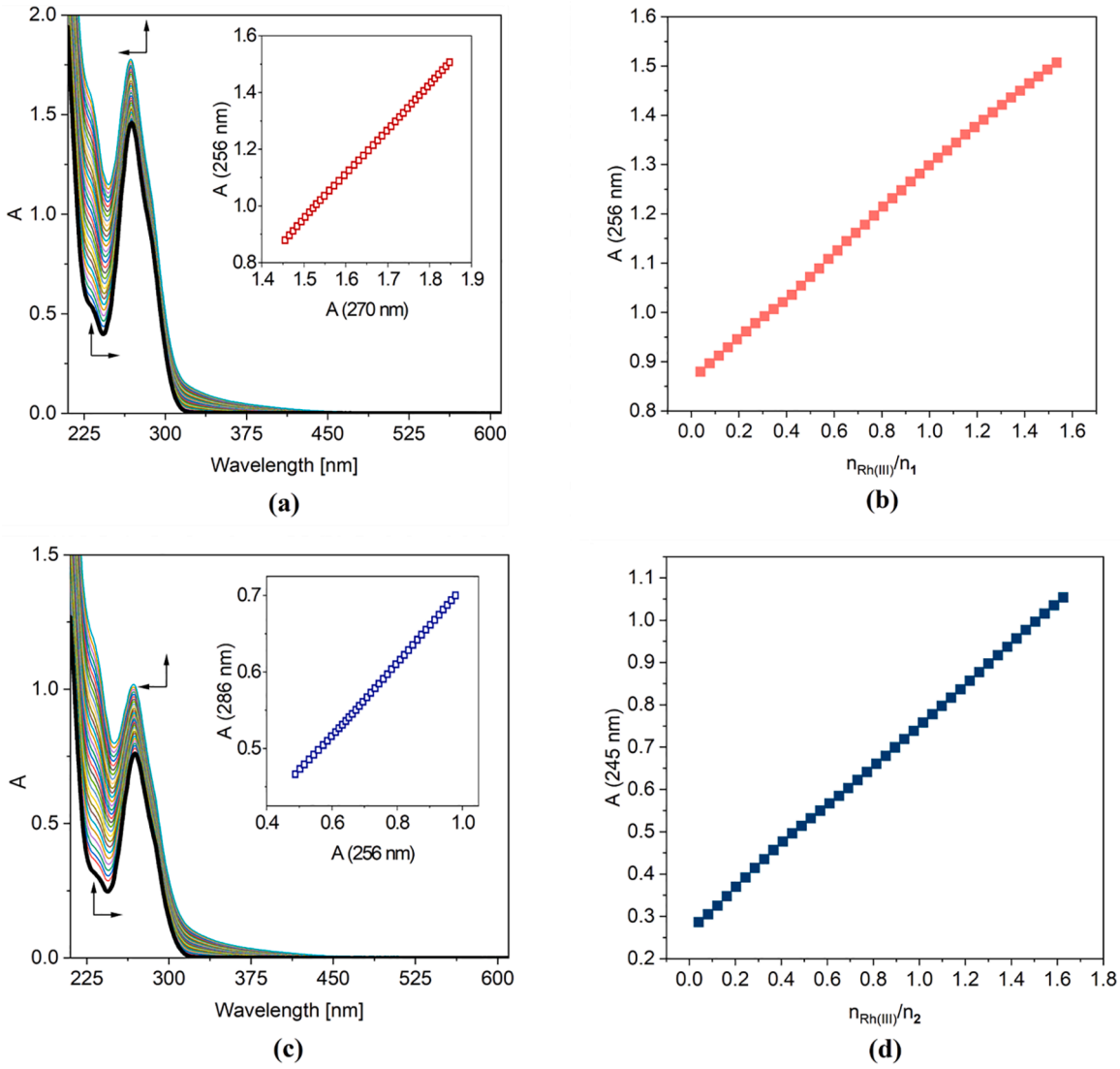

Fig. 6. The spectrophotometric titration results for the reaction of compounds (a-c) **1** ($C_1 = 5.78 \cdot 10^{-5}$ M) with Rh(III) ion ($C_{RhCl3} = 5.41 \cdot 10^{-4}$ M) and (d-e) **2** ($C_2 = 3.03 \cdot 10^{-5}$ M) with Rh(III) ion ($C_{RhCl3} = 2.89 \cdot 10^{-4}$ M) in MeOH solution: a, d) UV–Vis spectra; b, e) A-diagrams; c, f) absorbance *vs.* molar ratio $n_{Rh(III)}/n_n$.

Table 5
Stability constants values for Rh(III) complexes with **1** and **2** formed in MeOH together with their standard deviations. The values were obtained from spectrophotometric titration at room temperature.

Complex formula	Molar ratio	Coordination character	Ionic species of ligand	K_1	logβ
$[Rh(OH_2)_4HL^1]^{2+}$	1:1	bidentate	$(HL^n)^-$	$1.43 \cdot 10^7 \pm 8.12 \cdot 10^6$	7.15 ± 0.25
$[Rh(OH_2)_4HL^2]^{2+}$	1:1	monodentate	$(HL^n)^-$	$3.19 \cdot 10^6 \pm 7.24 \cdot 10^5$	6.50 ± 0.09

constants. They can be ordered according to their increasing stability as follows: $[Rh(OH_2)_4HL^1]^{2+} > [Rh(OH_2)_4HL^2]^{2+}$. In this case rhodium (III) forms a more stable complex with ligand **1**, than with **2**.

CRediT authorship contribution statement

Małgorzata Gawrońska: Conceptualization, Investigation, Visualization, Writing – original draft, Writing – review & editing. **Mateusz Kowalik:** Conceptualization, Investigation, Visualization, Writing – original draft, Writing – review & editing. **Joanna Duch:** Conceptualization, Investigation, Visualization, Writing – original draft. **Katarzyna Kazimierczuk:** Investigation, Writing – original draft. **Mariusz Makowski:** Conceptualization, Funding acquisition, Supervision, Writing – review & editing.

Declaration of Competing Interest

The authors declare that they have no known competing financial interests or personal relationships that could have appeared to influence the work reported in this paper.

Acknowledgments

This work was supported by a grant from the Polish National Science Centre (2019/33/B/ST4/00031). K. Kazimierczuk gratefully acknowledge the financial support for the X-ray diffraction measurement provided by SILICIUM SUPPORTING CORE R&D FACILITIES, DEC-2/2021/IDUB/V.6/S.

Appendix A. Supplementary data

Crystallographic data for structures **1** and **2** reported in this paper have been deposited with the Cambridge Crystallographic Data Centre as supplementary publications No. CCDC 2129928 and 2129928. Copies of the data can be obtained free of charge on application to CCDC, 12 Union Road, Cambridge CB2 1EZ, UK (Fax: (+44) 1223-336-033; Email: deposit@ccdc.cam.ac.uk). Supplementary data to this article can be found online at https://doi.org/10.1016/j.poly.2022.115865.

References

[1] R. Bentley, J. Ind. Microbiol. Biotechnol. 36 (2009) 775–786, https://doi.org/10.1007/s10295-009-0553-8.
[2] A. Kamal, M.N.A. Khan, K.S. Reddy, K. Rohini, G.N. Sastry, B. Sateesh, B. Sridhar, Bioorg. Med. Chem. Lett. 17 (2007) 5400–5405, https://doi.org/10.1016/j.bmcl.2007.07.043.
[3] A. Scozzafava, T. Owa, A. Mastrolorenzo, C.T. Supuran, Curr. Med. Chem. 10 (2003) 925–953, https://doi.org/10.2174/0929867033457647.
[4] C.T. Supuran, Curr. Pharm. Des. 14 (2008) 641–648, https://doi.org/10.2174/138161208783877947.
[5] K. Kumasaka, T. Kojima, S. Satoh, J. Pharm. Soc. Jap. 123 (2003) 1049–1054, https://doi.org/10.1248/yakushi.123.1049.
[6] A. Weber, A. Casini, A. Heine, D. Kuhn, C.T. Supuran, A. Scozzafava, G. Kiebe, J. Med. Chem. 47 (2004) 550–557, https://doi.org/10.1021/jm030912m.
[7] T. Gokcen, I. Gulcin, T. Ozturk, A.C. Goren, J. Enzyme Inhib. Med. Chem. 31 (2016) 180–188, https://doi.org/10.1080/14756366.2016.1198900.
[8] P.A. Masters, T.A. O'Bryan, J. Zurlo, D.Q. Miller, N. Joshi, Arch. Intern. Med. 163 (2003) 402–410, https://doi.org/10.1001/archinte.163.4.402.
[9] J. Prandota, Am. J. Ther. 8 (2001) 275–289, https://doi.org/10.1097/00045391-200107000-00010.
[10] A. Jönsson, B. Hallengren, T. Rydberg, A. Melander, Diabetes Obes. Metab. 3 (2001) 403–409, https://doi.org/10.1046/j.1463-1326.2001.00152.x.
[11] S.L. Greig, Drugs 76 (2016) 501–507, https://doi.org/10.1007/s40265-016-0559-2.
[12] S. Noble, K.L. Goa, Drugs 60 (2000) 1383–1410, https://doi.org/10.2165/00003495-200060060-00012.
[13] G.L. Plosker, K.F. Croom, Drugs 65 (2005) 1825–1849, https://doi.org/10.2165/00003495-200565130-00008.
[14] R.A. Alderden, M.D. Hall, T.W. Hambley, J. Chem. Educ. 83 (2006) 728–734, https://doi.org/10.1021/ed083p728.
[15] R. Confino-Cohen, A. Fishman, M. Altaras, A. Goldberg, Cancer 104 (2005) 640–643, https://doi.org/10.1002/cncr.21168.
[16] C.R. Culy, D. Clemett, L.R. Wiseman, Drugs 60 (2000) 895–924, https://doi.org/10.2165/00003495-200060040-00005.
[17] D. Armstrong, B. Bundy, L. Wenzel, H.Q. Huang, R. Baergen, L. Shashikant, L. J. Copeland, J.L. Walker, R.A. Burger, N. Engl. J. Med. 354 (2006) 34–43, https://doi.org/10.1056/NEJMoa052985.
[18] M. Offidani, A. Mele, L. Corvatta, M. Marconi, L. Malerba, A. Olivieri, S. Rupoli, F. Alesiani, P. Leoni, Leuk. Lymphoma 43 (2002) 1273–1280, https://doi.org/10.1080/10428190290026330.
[19] H.S. Pandha, L. Heinemann, G.R. Simpson, A. Melcher, R. Prestwich, F. Errington, M. Coffey, K.J. Harrington, R. Morgan, Clin. Cancer Res. 15 (2009) 6158–6166, https://doi.org/10.1158/1078-0432.CCR-09-0796.
[20] D. Knapp, N. Glickman, W. Widmer, Cancer. Chemother. Pharmacol. 46 (2000) 221–226, https://doi.org/10.1007/s002800000147.
[21] R. Singh, Z. Fazal, S.J. Freemantle, M.J. Spinella, Cancer Drug Resist. 2 (2019) 580–594. https://doi.org/10.20517/cdr.2019.19.
[22] C. Mascaux, M. Paesmans, T. Berghmans, F. Branle, J.J. Lafitte, F. Lemaitre, A. P. Meert, P. Vermylen, J.P. Sculier, Lung Cancer 30 (2000) 23–36, https://doi.org/10.1016/s0169-5002(00)00127-6.
[23] H.T. Arkenau, G. Chong, D. Cunningham, D. Watkins, B. Sirohi, I. Chau, A. Wotherspoon, A. Norman, A. Horwich, E. Matutes, Haematologica 92 (2007) 271–272, https://doi.org/10.3324/haematol.10737.
[24] R.P. Miller, R.K. Tadagavadi, G. Ramesh, W.B. Reeves, Toxins 2 (2010) 2490–2518, https://doi.org/10.3390/toxins2112490.
[25] L.E. Ta, L. Espeset, J. Podratz, A.J. Windebank, Neurotoxicology 27 (2006) 992–1002, https://doi.org/10.1016/j.neuro.2006.04.010.
[26] C.N. Morrison, K.E. Prosser, R.W. Stokes, A. Cordes, N. Metzler-Nolte, S.M. Cohen, Chem. Sci. 11 (2020) 1216–1225, https://doi.org/10.1039/C9SC05586J.
[27] M. Fandzloch, A.W. Augustyniak, L. Dobrzańska, T. Jędrzejewski, J. Sitkowski, M. Wypij, P. Golińska, J. Inorg. Biochem. 210 (2020), 111072, https://doi.org/10.1016/j.jinorgbio.2020.111072.
[28] N.P.E. Barry, P.J. Sadler, Chem. Soc. Rev. 41 (2012) 3264–3279, https://doi.org/10.1039/C2CS15300A.
[29] I. Omae, Coord. Chem. Rev. 280 (2014) 84–95, https://doi.org/10.1016/j.ccr.2014.07.019.
[30] M. Dobroschke, Y. Geldmacher, I. Ott, M. Harlos, L. Kater, L. Wagner, R. Gust, W. S. Sheldrick, A. Prokop, ChemMedChem 4 (2009) 177–187, https://doi.org/10.1002/cmdc.200800311.
[31] J. Markham, J. Liang, A. Levina, R. Mak, B. Johannessen, P. Kappen, C.J. Glover, B. Lai, S. Vogt, P.A. Lay, Eur. J. Inorg. Chem. 12 (2017) 1812–1823, https://doi.org/10.1002/ejic.201601331.
[32] G. Mansouri, M. Ghobadi, B. Notash, Inorg. Chem. Commun. 130 (2021), 108707, https://doi.org/10.1016/j.inoche.2021.108707.
[33] D.L. Ma, M. Wang, Z. Mao, C. Yang, C.T. Ng, C.H. Leung, Dalton Trans. 45 (2016) 2762–2771, https://doi.org/10.1039/C5DT04338G.
[34] C. Chuong, C.M. DuChane, E.M. Webb, P. Rai, J.M. Marano, C.M. Bernier, J. S. Merola, J. Weger-Lucarelli, Viruses 13 (2021) 980, https://doi.org/10.3390/v13060980.
[35] H.J. Zhong, W. Wang, T.S. Kang, H. Yan, Y. Yang, L. Xu, Y. Wang, D.K. Ma, C. H. Leung, J. Med. Chem. 60 (2017) 497–503, https://doi.org/10.1021/acs.jmedchem.6b00250.
[36] M. Kowalik, J. Brzeski, M. Gawrońska, K. Kazimierczuk, M. Makowski, CrystEngComm 23 (2021) 6137–6162, https://doi.org/10.1039/D1CE00869B.
[37] STOE & Cie GmbH. X-Area 1.75, Software Package for Collecting Single-Crystal Data on STOE Area-Detector Diffractometers, for Image Processing, Scaling Reflection Intensities and for Outlier Rejection; STOE & Cie GmbH: Darmstadt, Germany, 2015.
[38] G.M. Sheldrick, Acta Crystallogr. A 71 (2015) 3–8, https://doi.org/10.1107/S2053273314026370.
[39] O.V. Dolomanov, L.J. Bourhis, R.J. Gildea, J.A.K. Howard, H. Puschmann, J. Appl. Crystallogr. 42 (2009) 339–341, https://doi.org/10.1107/S0021889808042726.
[40] G.M. Sheldrick, Acta Crystallogr. C 71 (2015) 3–8, https://doi.org/10.1107/S2053229614024218.
[41] L.J. Farrugia, J. Appl. Crystallogr. 45 (2012) 849–854, https://doi.org/10.1107/S0021889812029111.
[42] K. Brandenburg, H. Putz, Diamond – Crystal and Molecular Structure Visualization Crystal Impact, 1997–2000. Rathausgasse 30, Bonn: GbR, Germany, 3.1 f.
[43] A. Chylewska, M. Ogryzek, R. Hałasa, A. Dąbrowska, L. Chmurzyński, M. Makowski, J. Coord. Chem. 17 (2014) 2885–2897, https://doi.org/10.1080/00958972.2014.953493.
[44] A. Okuniewski, D. Rosiak, J. Chojnacki, B. Becker, Polyhedron 90 (2015) 47–57, https://doi.org/10.1016/j.poly.2015.01.035.
[45] D. Rosiak, A. Okuniewski, J. Chojnacki, Polyhedron 146 (2018) 35–41, https://doi.org/10.1016/j.poly.2018.02.016.
[46] G.L. Perlovich, A.M. Ryzhakov, V.V. Tkachev, L.K. Hansen, Cryst. Growth Des. 11 (2011) 1067–1081, https://doi.org/10.1021/cg1012389.
[47] G.L. Perlovich, A.M. Ryzhakov, V.V. Tkachev, L.K. Hansen, O.A. Raevsky, Cryst. Growth Des. 13 (2013) 4002–4016, https://doi.org/10.1021/cg400666v.
[48] J. Bernstein, R.E. Davis, L. Shimoni, N.L. Chang, Angew. Chem. Int. Ed. Engl. 34 (1995) 1555–1573, https://doi.org/10.1002/anie.199515551.
[49] M. Károly, N. Béla, J. Pharm. Biomed. 130 (2016) 390–403, https://doi.org/10.1016/j.jpba.2016.03.053.
[50] D.T. Manallack, R.J. Prankerd, E. Yuriev, T.I. Oprea, D.K. Chalmers, Chem. Soc. Rev. 42 (2013) 485–496, https://doi.org/10.1039/c2cs35348b.
[51] G. Völgyi, R. Ruiz, K. Box, J. Comer, E. Bosch, K. Takács-Novák, Anal. Chim. Acta 583 (2007) 418–428, https://doi.org/10.1016/j.aca.2006.10.015.
[52] S. Sanli, Y. Altun, N. Sanli, G. Alsancak, J.L. Beltran, J. Chem. Eng. Data 54 (2009) 3014–3021, https://doi.org/10.1021/je9000813.
[53] K.Y. Tam, K. Takács-Novák, Anal. Chim. Acta 434 (2001) 157–167, https://doi.org/10.1016/S0003-2670(01)00810-8.
[54] E.K. Putra, R. Pranowo, J. Sunarso, N. Indraswati, S. Ismadji, Water Res. 43 (2009) 2419–2430, https://doi.org/10.1016/j.watres.2009.02.039.
[55] M. Mosquera, J.C. Penedo, M.C. Ríos Rodríguez, F. Rodríguez-Prieto, J. Phys. Chem. 100 (1996) 5398–5407, https://doi.org/10.1021/jp9533638.
[56] H. Nishiyama, H. Sakaguchi, T. Nakamura, M. Horihata, M. Kondo, K. Itoh, Organometaallics 8 (1989) 846–848, https://doi.org/10.1021/om00105a047.
[57] A. Petrović, M.M. Milutinović, E.T. Petri, M. Živanović, N. Milivojević, R. Puchta, A. Scheurer, J. Korzekwa, O.R. Klisurić, J. Bogojeski, Inorg. Chem. 58 (2018) 307–319, https://doi.org/10.1021/acs.inorgchem.8b02390.